Available online at www.sciencedirect.com
SCIENCE DIRECT
Polymer 47 (2006) 2904–2910
polymer
www.elsevier.com/locate/polymer

Calculating barrier properties of polymer/clay nanocomposites: Effects of clay layers

Bo Xu, Qiang Zheng *, Yihu Song, Yonggang Shangguan

Department of Polymer Science and Engineering, Zhejiang University, 38 Zheda Road, Hangzhou 310027, Zhejiang, People's Republic of China

Received 18 May 2005; received in revised form 11 February 2006; accepted 19 February 2006
Available online 10 March 2006

Abstract

We analyzed the effects of clay layers on the barrier properties of polymer/clay nanocomposites containing impermeable and oriented clay layers. Using the relative permeability theory in combination with the detour theory, we obtained new relative permeability expressions that allow us to investigate the relative permeability R_p as a function of lateral separation b, layer thickness w, gallery height H, layer length L, and layer volume fraction Φ_s. It was found that intercalated and/or incomplete exfoliated structures and dispersed tactoids with several layers can effectively enhance the barrier properties of the materials. Furthermore, we developed the chain-segment immobility factor to briefly discuss the chain confinement from clay layers. The results showed that the chain confinement enhanced the barrier properties of the intercalated nanocomposites. Our model is better consistent with the experiments when $\Phi_s > 0.01$. The findings provide guidelines for tailoring clay layer length, volume fraction and dispersion for fabricating polymer–clay nanocomposite with the unique barrier properties.

Keywords: Barrier properties; Polymer/clay nanocomposites

1. Introduction

Polymer/clay nanocomposites (PCN) with low clay loading are novel materials used as high-barrier packaging products for food and electronics [1–4]. Such materials typically consist of nano-scaled silicate layers dispersed in a polymer matrix, consisting of which the clays belong to the general family of 2:1 layer- or phyllo-silicates, such as montmorillonite, saponite, synthetic mica, etc. composed of stacked silicate layers of approximately 10–2000 nm in length and 1 nm in thickness [1–7]. Experimental results showed dispersed silicate layers with the aspect ratio as high as 10–2000 lead to the unique barrier property of PCN [3–7]. Unfortunately, because of great challenges in preparing PCN, it is difficult to understand the effects of clay layers on barrier properties of these materials.

Considerable efforts have been focused on correlating and predicating barrier properties of polymeric composite materials filled with whiskers (fibers, the filled polymer systems, carbon nanotubes, cellulose, etc.), or plate-like inorganic fillers (talcum, clay, mica, etc.) [7–9,11,12]. The detour theory of Nielsen was provided for predicting the permeability of conventional composites [8]. An analytical model for the barrier properties of oriented cubic composites was developed by Fredrickson and Bicerano [13]. This model extended the previous work to examine disorder and polydispersity effects, and accounted fully for an improved equation which is valid over a much wider concentration range. Based on the numerical simulation method of Gusev [14], three-dimensional periodic computer models introduced by Gusev and Lusti [15] evaluated barrier properties of nanocomposites comprised of perfectly aligned randomly dispersed dish-like platelets. For the PCN, Bharadwaj [12] showed that the Nielsen's formula could be modified to demonstrate the relationship between gas barrier property with the length and relative orientation of silicate layers, and the state of filler aggregation. As a result, the theoretical strides have been made progress in analyzing the permeability reduction engendered from dispersion of fillers.

Evaluating the permeability of materials, on the other hand, requires an investigation on the transformations of a polymer matrix which result in changes of the local gas permeability coefficient [16–20]. In the PCN, the transformations of a polymer matrix caused by the presence of the nanometer-scaled clay layers, have been widely studied. Compared with the conventional composites, the chain-segment immobility in the PCN (especially the intercalated) increases to a certain

* Corresponding author. Tel./fax: +86 571 87952522.
E-mail address: zhengqiang@zju.edu.cn (Q. Zheng).

0032-3861/$ - see front matter © 2006 Elsevier Ltd. All rights reserved.
doi:10.1016/j.polymer.2006.02.069

extend in the confined environment provided by the clay layers [21,22], which is suggested as an increase in the glass transition temperature (T_g) of poly(styrene-*b*-butadiene) copolymer [23], poly(butylene terephthalate) [24], polypropylene [25], polymethylphenylsiloxane [26], etc. What are the influences of the change of the polymer matrix on permeabilities of PCN? Furthermore, the dispersed clay layers sometimes affect the nature of the crystallization, resulting in transformation of the crystal form and the crystallinity [27], and a decrease in the crystallite size [28]. In general, the latter is also influenced from annealing. Thus, we only consider the former transformation here and ignore the latter. Additionally, according to X-ray diffraction (XRD) data and transmission electronic spectroscopy (TEM) [1–10], one can easily obtain the extraordinarily important parameter discerning the dispersion of clay layers—the spacing between diffractional lattice planes in PCN. Clearly, the previous analytical and numerical models rarely elucidate these influences and hardly utilize this parameter. The present paper attempts to fill in some of the gaps in our understanding.

In this study, we combine, for the first time, the relative permeability theory of semi-crystalline polymers [16–20] with the detour theory [8] to evaluate the relative permeabilities of PCN. We propose a model to calculate the factor of the detour ratio, incorporate Michaels–Bixler formula [17]—chain-segment immobility factor into our model, and then obtain the new relative permeability expressions for PCN. We focus in great detail on discussing the effects of clay layers, including the layer length, clay loading, the layer dispersion, and the chain confinement on the barrier properties in PCN assuming no change in the nature of the crystallizations.

2. Model

In order to investigate the relative permeabilities of PCN, we assumed the individual clay layers as cuboids with length and width L and thickness w [13,29,30]. The PCN are simply viewed as the crystal ordering of clay layers dispersing in a polymer (shown in Fig. 1), which leads to the maximized barrier properties and are therefore of most interest to applications. Assuming silicate layers are considered as crystalline lamellas in the matrix in a semi-crystalline polymer based on Klute's theory [16–18], we estimate the permeability P for PCN as

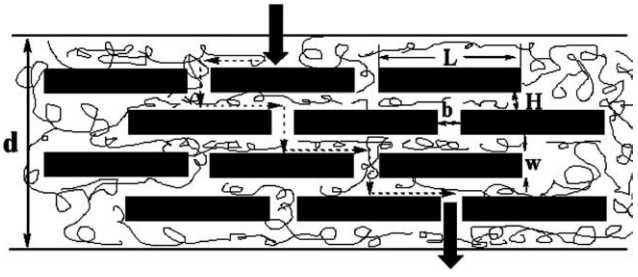

Fig. 1. Crystalline structure of cuboid silicate layers dispersed in a matrix as similar to Kuznetsov and Balazs' model [31]. The arrow presents the path of a penetrant through a PCN film.

$$P = P_0(1-\Phi_s)\zeta(\Phi_s) \tag{1}$$

where P_0, Φ_s and ζ are the permeability of the matrix in PCN, the clay layers volume fraction and a function for the reduction of permeability due to clay layers in the polymer matrix, respectively. Thus, the relative permeability for PCN can be obtained as the following equation:

$$R_p = (1-\Phi_s)\zeta(\Phi_s) \tag{2}$$

Owing to silicate layers dispersed in the films, a penetrant has to bypass clay layers and move through amorphous region of PCN, leading to a decrease in permeability. Moreover, the mobility of polymer chain segments in the PCN is obviously different from pure polymer due to confined geometry environment [21,31], which affects the gas permeability. Thereby, we are considering two factors for the permeability reduction, namely the factor of polymer chain-segment immobility, ζ_1, and the factor of the detour ratio, ζ_2, which can be defined as the ratio of the film thickness, d, in nominal diffusion flow direction to average length of the diffusion tortuous distance between silicate layers. According to the ideas in Refs. [16,17], we present ζ as a function of Φ_s as follows

$$\zeta(\Phi_s) = \frac{\zeta_2(\Phi_s)}{\zeta_1} \tag{3}$$

To evaluate ζ_2, we developed a model based on the detour argument in the Nielsen's theory [8]. Due to their high aspect ratio, silicate layers are easily exposed to orient ordering at a low volume fraction in the melt extrusion. The crystalline structure for the exfoliated PCN can be obtained in the casting films [32], which is just similar to the one shown in Fig. 1. The traveling tortuous distance may be given as

$$d' = d_a + d \tag{4}$$

where d_a is obligatory traveling path of a penetrant through a film corrected with regard to the thickness due to filled silicate layers. In term of Vincent and co-workers' equation [33], we can illuminate our model as

$$(L+b)^2(w+H) = \frac{L^2 w}{\Phi_s} \tag{5}$$

Here, b and H are the lateral separation (edge-to-edge distance) and the separation gap between adjacent cuboids (face-to-face distance), respectively. We denote the average number of cuboid layers which a penetrant must go around by $N_p = d/(w+H)$. Additionally, the penetrant has to penetrate a certain lateral separation between adjacent cuboids throughout a film. The distance d_T of the lateral separation should not be ignored in calculating the path distance d_a. For example, $b = 30$ nm was evaluated in the maleated polyethylene–clay nanocomposites by TEM [34]. Compared to $L = 140$ nm, b should be regarded. Considering $d_T = b/2$ as shown in Fig. 1, we present the path distance d_a as

$$d_a = N_p\left(\frac{L}{2} + d_T\right) = \frac{d}{w+H}\frac{L+b}{2} \tag{6}$$

Then, we obtain the detour ratio as

$$\zeta_2(\Phi_s) = \frac{d}{d'} = \frac{1}{1 + \frac{L}{2w}\left(1 + \frac{b}{L}\right)^3 \Phi_s} \tag{7}$$

From Eqs. (2), (3) and (7), the relative permeability R_p is given by

$$R_P = \frac{(1-\Phi_s)/\zeta_1}{1 + \frac{L}{2w}\left(1 + \frac{b}{L}\right)^3 \Phi_s} \tag{8}$$

Combining Eqs. (5) and (8), R_p can also be expressed as

$$R_P = \frac{(1-\Phi_s)/\zeta_1}{1 + \frac{L}{2}\left(\frac{w}{\Phi_s}\right)^{1/2}(w+H)^{-3/2}} \tag{9}$$

3. Comparison with other models

Nielsen formulated a detour model for the circular or rectangular filler particles, which may be compared with the present model for cuboid layers. In case that $b \ll L$, and $\zeta_1 = 1$, our equation is similar to Nielsen's formula, namely:

$$R_P = \frac{1-\Phi_s}{1 + \frac{L}{2w}\Phi_s} \tag{10}$$

Hence, the Nielsen's formula is appropriate in the condition of not only the clay layers with high aspect ratio and no confinement on a polymer matrix, but also the dilute dispersions discussed by Gusev and Lusti [14,15].

Fredrickson and Bicerano explicitly estimated the detour factor for randomly positioned cuboid particles of uniform size and shape, and provided a crossover formula to interpolate between the asymptotic dilute and semi-dilute regimes [13]. The finite-element based methodology was successfully adopted for predicting effects of the platelet aspect ratio and the volume fraction on the transport properties of nanocomposites by Gusev and Lusti [15]. Both models account for influences from the inherent characters of fillers on the permeability reduction of composites. Moreover, we take into account the dispersion of fillers and the chain confinement in our model, which increases considerably the complexity of our equations.

Fig. 2 compared our predictions obtained in this model with those of the four selected literature models. All methods predicted comparable improvement in the barrier properties (permeability reductions) for the layer aspect ratio (namely, the layer length) of up to 500, but our model predicts much greater potential enhancements at layer aspect ratio of the range from 10 to 300 than are expected based on the other models (see the inset of Fig. 2). Moreover, considering the chain-segment immobility factor, $\zeta_1 > 1$, the relative permeability should be lower than that at $\zeta_1 = 1$. Additionally, the Cussier–Aris model and Gusev–Lusti model meet difficulty to predict the barrier properties for the layer aspect ratio of about 2 due to the geometric factor estimated by Fredickson and Bicerano.

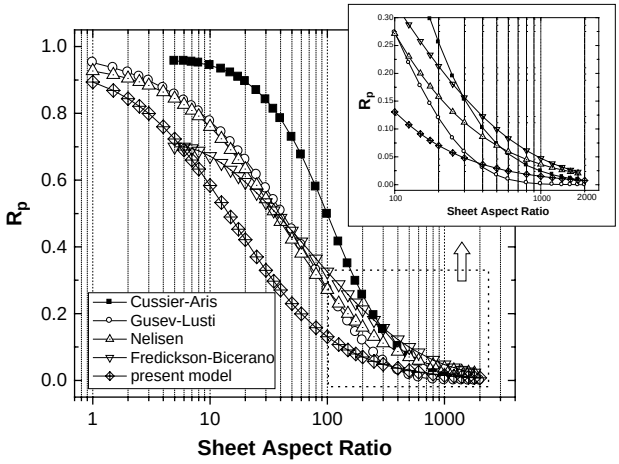

Fig. 2. Comparison of predictions for the relative permeability R_p as a function of layer aspect ratio; Φ_s is the layer volume fraction and $a = L/w$ the aspect ratio. We compare our Eq. (9) with $w = 1$, $H = 10$ nm at $\Phi_s = 0.05$, and no changes of the matrix and four literature formulae currently used for permeability predictions: the Nielsen formula $R_p = (1-\phi_s)/(1+a/2)$ [8], modified Cussler–Aris formula $R_p = 1/(1+\mu a^2\phi_s^2)$ with the geometric factor $\mu = \pi^2/[4\ln(a/2)]^2$ advocated elsewhere [13], the Fredrickson–Bicerano composite formula $R_p = [1/(2+a_1\kappa a\phi_s) + 1/(2+a_2\kappa a\phi_s)]^2$ with $a_1 = (2-\sqrt{2})/4$, $a_1 = (2+\sqrt{2})/4$, and $\kappa = \pi/\ln(a/2)$ and the Gusev–Lusti formula $R_p = \exp[-(a\Phi_s/x_0)^\beta]$ with least-square parameter $\beta = 0.71$ and $x_0 = 3.47$ [13]. The inset shows the range of layer aspect ratio from 100 to 2000.

4. Discussion

4.1. Unconfined matrixes ($\zeta_1 = 1$)

First we consider the case that $\zeta_1 = 1$, assuming that the silicate layers have no effect on polymer chain-segment immobility. b should be less than L in Fig. 1. Otherwise, the penetrant directly diffuses throughout the lateral separation. When $b = 0$, the penetrant could diffuse along the plane of silicate layer and get out from the lateral plane of the composite film. This situation is beyond the interest of this paper. To study the influence of b on R_p, we set Φ_s as a typical value 0.03, which is near the threshold volume fraction for the properties of PCN. The relative permeability profiles for various L are shown in Fig. 3. It can be seen that increasing L and b leads to decreases in the values of R_p. Experimentally, water relative permeability decreases drastically for polyimide nanocomposites, with 2 wt% of hectrite ($L = 46$ nm), saponite (165 nm), montmorillonite (218 nm), and synthetic mica (1230 nm) [2]. When $L > 150$ nm, R_p is independent on b, indicating that the relative permeabilities are sensitive to the lateral separation only when the length is small, vice versa. As Eq. (8) is close to Nielsen's equation for the long layers, it is easy to understand that the experimental result is comparatively consistent with the calculated value by Nielsen's equation for the polyetherimide hybrid filled with the montmorillonite of $L = 218$ nm [2].

Nanometer-scaled dispersion of silicate layers with the large aspect ratio is a key to improve the certain properties of PCN, especially high barrier. However, aggregation of silicate layers in a polymer leads to a decrease in the aspect ratio, deteriorating the barrier of PCN. Therefore, the experimental

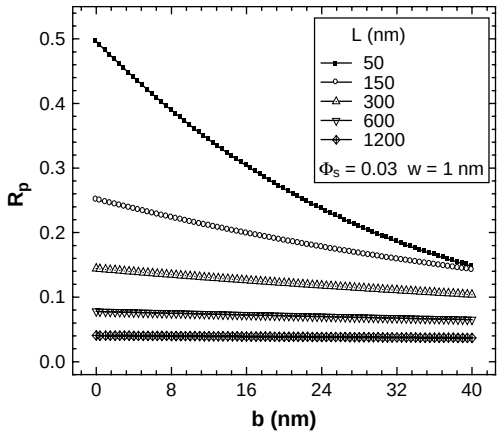

Fig. 3. Relative permeability as a function of the lateral separation obtained from Eq. (8) when $\zeta_1=1$, $\Phi_s=0.03$ and $w=1$ nm for five different values of layer lengths noted in the legend. We assumed that the under boundary of b is equal to 0 and the up boundary cannot be beyond L.

values for water vapor permeability are higher than the calculated one based on Nielsen's equation due to the agglomerate of hectrite and non-homogeneous dispersion of saponite in the hybrids [2].

Generally, the d_{001} spacing of the organically modified clay ranges from 1.5 to 2.5 nm. It is assumed that no penetrant can permeate the galleries of layer aggregations, but flow through the gaps between aggregations. Experimental results showed the gallery height could range from about 4 nm for the intercalated nanocomposites to about 200 nm for the exfoliated ones [21,34]. Fig. 4 presented the calculated values of R_p according to Eq. (9) for various gallery heights and a typical value of $L=150$ nm. The set values in Fig. 4 are close to the actual experiment results. For the same silicate layer volume content, the different gallery heights should correspond with different systems which the matrixes have different intercalation capacities [25,35], or the different organoclays [36]. As increasing the volume contents of organically modified montmorillonite blended with maleated polyethylene, the nanocomposites show the structures from the disordered and exfoliated for 9 vol%, to the ordered and exfoliated for 12–18 vol%, to the intercalated and exfoliated coexist for 21–24 vol% and the intercalation above 27 vol% [34]. The relative permeability increases with an increase in H at a given w. The arrows represent the shift trend of R_p with w in curves. When $H<9$ nm, increasing the thickness of the multilayer layers only results in an increase in R_p, whereas R_p shows a sharp decrease in the case of $H>150$ nm. In the intermediate, increasing w leads to an improvement in barrier properties and then a deterioration after a certain w. It is clear that certain multilayer layers or tactoids facilitate to effectively enhance the barrier for the exfoliated PCN, while R_p hardly alters when w is less than 20 nm for the intercalated. In other word, the barrier properties of the exfoliated PCN are more perfectly sensitive to the stack of clay layers than those of the intercalated.

As an important parameter, H characterizing the degree of exfoliation of silicate layers can be measured by WAXD and TEM [2,4,34]. Increasing Φ_s leads to a decrease in H. Thus, we assume that increasing Φ_s leads to $H=200$, 100, 50, 20, 9, and 4 nm, respectively [35]. Fig. 5 reflects a function of the multilayer thickness at condition of various fractions ($\Phi_s=$ 0.005, 0.01, 0.03, 0.05, 0.10, and 0.15), indicating that increasing Φ_s can enhance the barrier property at the same w. Φ_s affects extensively R_p of PCN at $\Phi_s\leq 0.05$. It is easier to understand that increasing Φ_s (>0.05) almost has no effect on R_p, and even leads to increases in R_p due to deterioration of dispersion and exfoliation of the clay layers for PCN [3,4]. As shown in the trend of R_p by the arrows, high Φ_s increases the dependence of the barrier properties of PCN on the dispersion of the clay layers.

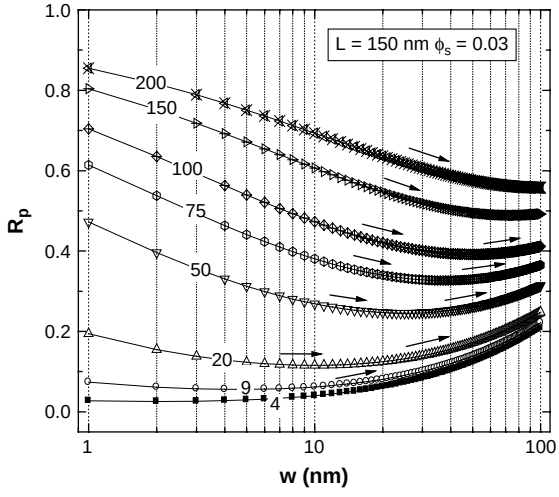

Fig. 4. Relative permeability as a function of the agglomerate width obtained from Eq. (9) for various gallery heights at $L=150$ nm, $\zeta_1=1$, and $\Phi_s=0.03$. Here, we consider that H shown on the lines represents the distance between agglomerations or silicate particles, namely the studied systems are intercalated and exfoliated complexes. The agglomeration width is equivalent to the thickness of one layer to scores of layers.

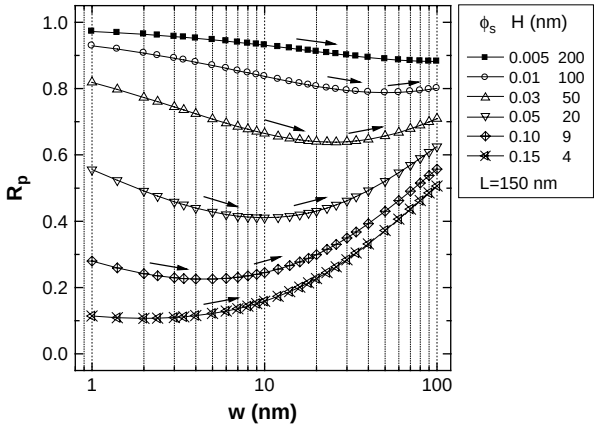

Fig. 5. Relative permeability as a function of the agglomerate width obtained from Eq. (9) for various clay layer volume fraction with the corresponding gallery heights at $L=150$ nm. Here, we consider the meaning of H and w as that of Fig. 4.

4.2. Confined matrixes ($\zeta_1 \neq 1$)

It should be noted that the above analysis is based on the assumption $\zeta_1 = 1$. However, the mobility of polymer chain-segments is considerably reduced in the confined environment provided by the silicate layers. Unfortunately, very few exact results are known for ζ_1. We introduce the chain-segment immobility factor $\zeta_1 > 1$ by virtue of studies on dealing with effects of crystallization on a diffusion constant [17,18]. After systematic experiments, authors in Refs. [17,18] obtained the chain-segment immobility factor from the systemic studies on gas molecules penetrating the polyethylene films of different crystallinities on basis of Brandt's formula [37]. The chain-segment immobility factor can be written as

$$\zeta_1 = \exp[k(D - \Phi_L^{1/2}/2)]^2 \tag{11}$$

where k is a constant for different penetrants diffused through the same film, D is the diameter of a penetrants, and $\Phi_L^{1/2}/2$ is approximately equal to mean unoccupied distance between two chain segments. Increasing the volume fraction (Φ_c) of crystallinity of polyethylene leads to a decrease in the chain-segment immobility and thereby an improvement of barrier property. For nitrogen, the chain-segment immobility factor of polyethylene is 1.1, 1.2 and 2.0 at $\Phi_c = 0.29$, 0.43 and 0.77, respectively.

Experimental results in many polymer–clay nanocomposite systems show that more clay layers cause more reduction in chain-segment mobility [23–26,38,39]. In our model, more clay layers lead to a decrease in H. Theoretical calculations also exhibit that, decreasing H results in entropic penalty of polymer confinement [21,22,29–31], that is to say, more reduction in chain-segment mobility. Although clay layers and polymer lamellar crystallites are not in complete agreement, it is safe to assume that the effect of the clay layers is similar to that of lamellar crystallites on the segment immobility of confined polymer chains. Therefore, in expression (11) for our model, $\Phi_L^{1/2}/2$ decreases as Φ_s increases and then ζ_1 increases. Thus, R_p reduces drastically, especially for the intercalated PCN with high Φ_s, where the chain-segment becomes more immobile due to much more confined geometry compared with the exfoliated PCN. Also, we calculate relative permeability for various ζ_1 and $\zeta_1 = 1$, respectively, from Eq. (9). As shown in Table 1, the relative permeability should be attached importance to the chain-segment immobility factor. In particular, R_p reduces drastically as ζ_1 increase from the exfoliated PCN to the intercalated. Unfortunately, for PCN, more systematic experimental studies on the influence of ζ_1 to R_p are needed to test our predictions.

Table 1
Effect of chain-segment immobility factor on relative permeability

Volume fraction[a] Φ_s	Gallery height[a] H (nm)	Segment immobility factor[b] ζ_1	Relative permeability	
			R_p	R_p ($\zeta_1 = 1$)
0.005	200	1.0	0.993	0.993
0.01	100	1.1	0.887	0.986
0.03	50	1.4	0.674	0.963
0.05	20	1.7	0.559	0.9301
0.10	9	2.0	0.431	0.862
0.15	4	5.0	0.154	0.771

[a] Gallery height assumed as in Fig. 5.
[b] Segment immobility factor is assumed in term of Michaels and Bixler's results [17], and $\zeta_1 = 1$ represents no confinement of chain segments.

4.3. Comparison of the calculated R_p and the experimental

As a result of the dispersed clay layers, it has been experimentally and numerically proved that the gas barrier properties have been improved dramatically in PCN [1–4,8,13]. As shown in Table 2, the gas barrier properties of polyimide and polyester–clay nanocomposites have been investigated in detail. In term of the provided TEM micrographs and the discussion in the corresponding references, we obtain effective layer lengths in these nanocomposites.

Fig. 6 shows the relationship of the relative permeability and the volume fraction of clay layers calculated using Eq. (8). Considering the dispersion degree of clay layers, we can deduce that higher exfoliation degree of clay leads to higher aspect ratio, and longer dispersed layers, smaller lateral separation b in our model. Therefore, we calculate the curves shown in Fig. 6, based on practically designing the parameters of L, b, w and ζ_1.

Based on Ref. [1a], we set $L = 200$ nm and $w = 1$ nm. The calculated result is well consistent with the experimental data for polyester nanocomposites filled with montmorillonite of various contents. Moreover, our calculated value of $L = 218$ and $b = 2$ is in agreement with the relative permeability of

Table 2
Relative permeability of PCN and their relate parameters in references

Clay	Clay volume fraction Φ_s (%)[a]	Relative permeability R_p	Effective length L (nm)[b]	Reference
Montmorillonite	0.5	0.80	200	[3]
	1.4	0.37	200	
	2.8	0.54	750	
	5.8	0.38	750	
Montmorillonite	0.58	0.71	200	[1a]
	1.16	0.50	200	
	1.75	0.30	200	
	2.95	0.28	200	
	4.78	0.15	200	
Hectrite	1.16	0.95	46	[2]
Saponite	1.16	0.78	165	
Montmorillonite	1.16	0.44	218	
Synthetic mica	1.16	0.08	1230	

[a] The calculation is based on the density of pristine clay, 2.6 g/cm^3 [40,41]; and polyimide, 1.5 g/cm^3 [41], and polyester density, 1.1 g/cm^3 [3].
[b] Layer length means the length of the organophilic clay multilayer in the intercalated nanocomposites and that of the monolayer in the exfoliated.

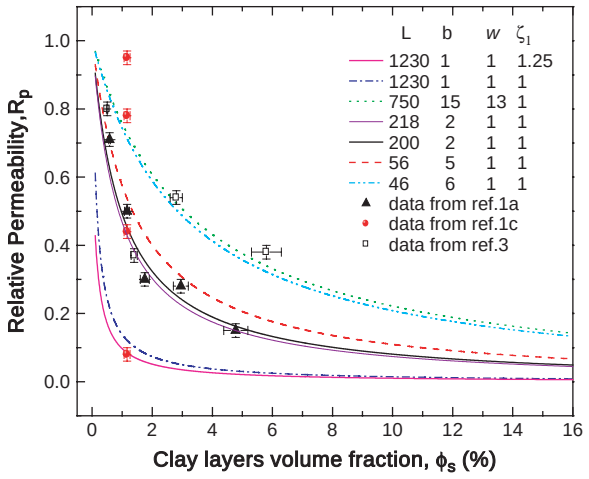

Fig. 6. Comparison of calculated relative permeability with experimental data of polyimide–clay and polyester–clay nanocomposites in Refs. [1a–3]. The signs(▲,●,□) represent the experimental data. The calculated fits based on Eq. (8) for different L, b, w and ζ_1 are also shown. Here L means the same as that in Table 2.

2 wt% montmorillonite filled polyimide nanocomposite shown in Ref. [1c]. For the synthetic mica system, the calculated R_p is higher than the experimental one without considering the chain-segment immobility ($\zeta_1=1$). Actually the polyamide chains show the higher elastic modulus in the synthetic mica composite of such longer layers as compared to hectrite, saponite and montmorillonite composites, indicating more chain-segment confinement in this composite. Therefore, the calculated value is well consistent with the experimental one at $\zeta_1=1.25$. For hectrite and saponite composites, experimental results are obviously higher than calculated ones at low effective length, suggestive of poor dispersion of clay layers. Additionally, our calculated R_p at $L=750$, $b=15$ and $w=13$ is in agreement with the experimental R_p of 5 and 10 wt% montmorillonite nanocomposites in Ref. [3]. R_p of 1 wt% montmorillonite nanocomposites is much higher than the calculated one at $L=200$ and $b=2$, while consistent at the same parameters in 2.5 wt% montmorillonite nanocomposite. The results perhaps derive from the limitation of our ideal model. Less clay layers in the actual samples can not be formed as the idealized arrangement of clay layers in our model. However, more clay layers can easily be arranged as the structure of our model. Therefore, our model has its limitation for the less clay layers filled systems. As shown in Fig. 6, our model is better consistent with the experiment when $\Phi_s>0.01$.

5. Conclusion

We developed the relative permeability theory and the detour theory to study the effects of clay layers in the barrier properties of PCN. To calculate the detour ratio, we took into account the crystal ordering of clay layers and obtained the relative permeability expressions. We systematically investigated the relative permeability of PCN dependent on the characteristic of clay layers—dispersion, layer thickness, gallery height, layer length, layer volume fraction, and chain-segment immobility factor. In addition, we developed the chain-segment immobility factor to model the chain confinement provided by clay layers, and briefly discuss effects of the chain-segment immobility on the barrier properties of PCN.

Increasing the lateral separation resulted in a decrease in relative permeability, especially for the PCN with the shorter layers. Intercalated or incomplete exfoliated structures with certain multilayer layers, and/or the chain confinement provided by clay layers could effectively enhance the barrier property of the materials, while increasing Φ_s (>0.05) or layer length ($L>500$ nm) hardly results in any improvement of the barrier property. Furthermore, exfoliated structure with stacks of several clay layers and intercalated morphology without tactoids will be beneficial to the materials with high barrier properties. By comparing the expressed experimental results, our model is better consistent with the experiment when $\Phi_s>0.01$.

We believe that the predictions presented here can be used as new guidelines for designing and developing PCN with unique barrier permeability, and the developed theory can be easily applied to other polymer-filler systems. Additionally, in virtue of the diffusion of molecules, our theory provides a possibility to study polymer morphology in PCN.

Acknowledgements

The present work was financially supported by National Science Fund for Distinguished Young Scholars (grant 50125312), National Basic Research Program of China (grant 2005 CB 623800) and National Natural Science Foundation of China (grant 50373037). The authors thank the reviewers for providing their valuable advice regarding the developed models of the barrier properties of polymer–nanoparticle composites and the chain-segment immobility factor, and Dr Yong He from Toray Fibers and Textiles Research Laboratories (China) Co., Ltd for his helpful discussions.

References

[1] (a) Yano K, Usuki A, Okada A, Kuruachi T, Kamigaito O. J Polym Sci, Part A: Polym Chem 1993;31:2493.
(b) Messersmith PB, Giannelis EP. J Polym Sci, Part A: Polym Chem 1995;33:2289.
[2] Yano K, Usuki A, Okada A. J Polym Sci, Part A: Polym Chem 1997;35:2289.
[3] Bharadwaj RK, Mehrabi AR, Hamilton C, Trujillo C, Murga M, Fan R, et al. Polymer 2002;43:3699.
[4] Kojima Y, Fukumori K, Usuki A, Okada A, Kurauchi T. J Mater Sci Lett 1993;12:889.
[5] (a) Sheng N, Boyce MC, Parks DM, Rutledge GC, Abes JI, Cohen RE. Polymer 2004;45:487.
(b) Cabedo L, Giménez E, Lagaron JM, Gavara R, Saura JJ. Polymer 2004;45:5233.
[6] (a) Messermith PB, Giannelis EP. J Appl Polym Sci 1995;33:1047.
(b) Thellen C, Orroth C, Froio D, Ziegler D, Lucciarini J, Farrell R, et al. Polymer 2005;46:11716.
(c) Yu YH, Lin CY, Yeh JM, Lin WH. Polymer 2003;44:3553.
[7] Barrer RM, Barrie JA, Raman NK. Polymer 1962;3:605.

[8] Nielsen LE. J Macromol Sci Chem 1967;5:929.
[9] Petropoulos JH. J Polym Sci, Part B: Polym Phys 1985;23:1309.
[10] (a) Ganguli S, Dean D, Jordan K, Price G, Vaia R. Polymer 2003;44: 6901.
(b) Chastek TT, Stein A, Macosko C. Polymer 2005;46:4431.
[11] (a) Ward WJ, Gaines GL, Alger MM, Stanley TJ. J Membr Sci 1991;53: 173.
(b) Cai Z, Berdichecsky AL. Polym Compos 1993;14:314.
[12] Bharadwaj RK. Macromolecules 2001;34:9189.
[13] Fredrickson GH, Bicerano J. J Chem Phys 1999;110:2181.
[14] Gusev AA. Macromolecules 2001;34:3081.
[15] Gusev AA, Lusti HR. Adv Mater 2001;13:1641.
[16] Klute CH. J Appl Polym Sci 1959;1:340.
[17] Michaels AS, Bixler HJ. J Polym Sci 1961;50:413.
[18] Michaels AS, Vieth WR, Barrie JA. J Appl Phys 1963;34:13.
[19] Hiltner A, Liu RYF, Hu YS, Baer E. J Polym Sci, Part B: Polym Phys 2005;43:1047.
[20] Kofinas P, Cohen RE, Halasa AF. Polymer 1994;35:1229.
[21] Balazs AC, Singh C, Zhulina E. Macromolecules 1998;31:8370.
[22] Lyatskaya Y, Balazs AC. Macromolecules 1998;31:6676.
[23] Laus M, Francesangeli O, Sandrolini F. J Mater Res 1997;12:3134.
[24] Chisholm BJ, Moore RB, Barber G, Khouri F, Hempstead A, Larsen M, et al. Macromolecules 2002;35:5508.
[25] Kawasumi M, Hasegawa N, Kato M, Usuki A, Okada A. Macromolecules 1997;30:6333.
[26] Anastasiadis SH, Karatasos K, Vlachos G, Giannelis EP, Manias E. Phys Rev Lett 2000;84:915.
[27] (a) Vaia RA, Vasudevan S, Krawiec W, Scanlon LG, Giannelis EP. Adv Mater 1995;7:154.
(b) Liu LM, Qi ZN, Zhu XG. J Appl Polym Sci 1999;71:1133.
(c) Wu QJ, Liu XH, Berglund LA. Polymer 2002;43:2445.
[28] Messersmith PB, Giannelis EP. J Polym Sci, Part A: Polym Chem 1995; 33:1047.
[29] Ginzburg VV, Balazs AC. Macromolecules 1999;32:5681.
[30] Ginzburg VV, Singh C, Balazs AC. Macromolecules 2000;33:1089.
[31] Kuznetsov DV, Balazs AC. J Chem Phys 2000;112:4365.
[32] Celzard A, Mareche JF, Furdin G, Puricelli S. J Phys D: Appl Phys 2000; 33:3094.
[33] Jennifer M, Saunders JW, Goodwin RM, Vincent B. J Phys Chem B 1999; 103:9211.
[34] Koo CM, Ham HT, Kim SO, Wang KH, Chung IJ, Kim DC, et al. Macromolecules 2002;35:5116.
[35] (a) Park CI, Park OO, Lim JG, Kim HJ. Polymer 2001;42:7465.
(b) Fornes TD, Yoon PJ, Keskkula H, Paul DR. Polymer 2001;42:9929.
(c) Fornes TD, Hunter DL, Paul DR. Polymer 2004;45:2321.
[36] (a) Fornes TD, Yoon PJ, Hunter DL, Keskkula H, Paul DR. Polymer 2002;43:5915.
(b) Yoon PJ, Hunter DL, Paul DR. Polymer 2003;44:5323.
(c) Fornes TD, Hunter DL, Paul DR. Macromolecules 2004;37:1793.
[37] Brandt WW. J Phys Chem 1959;63:1080.
[38] Giannelis EP. Adv Mater 1996;6:29.
[39] Lan T, Pinnavaia T. J Chem Mater 1994;6:2216.
[40] Krishnamoorti R, Giannelis EP. Macromolecules 1997;30:4097.
[41] Kashiwagi T, Harris Jr RH, Zhang X, Briber RM, Cipriano BH, Raghavan SR, et al. Polymer 2004;45:881.